Supporting information

Multifunctional fluorescent leucomalachite green derivatives for chemodosimetric detection of Fe^{3+}, specific imaging of lipid droplets and intracellular pH monitoring

Thekke Thattariyil Divya[a], Darpan Raghav[b], Krishnan Rathinasamy[b]*, Lakshmi Chakkumkumarath[a]*

a. Department of Chemistry, National Institute of Technology Calicut, Kerala, India-673601

b. School of Biotechnology, National Institute of Technology Calicut, Kerala, India-673601

Corresponding Author: lakshmic@nitc.ac.in

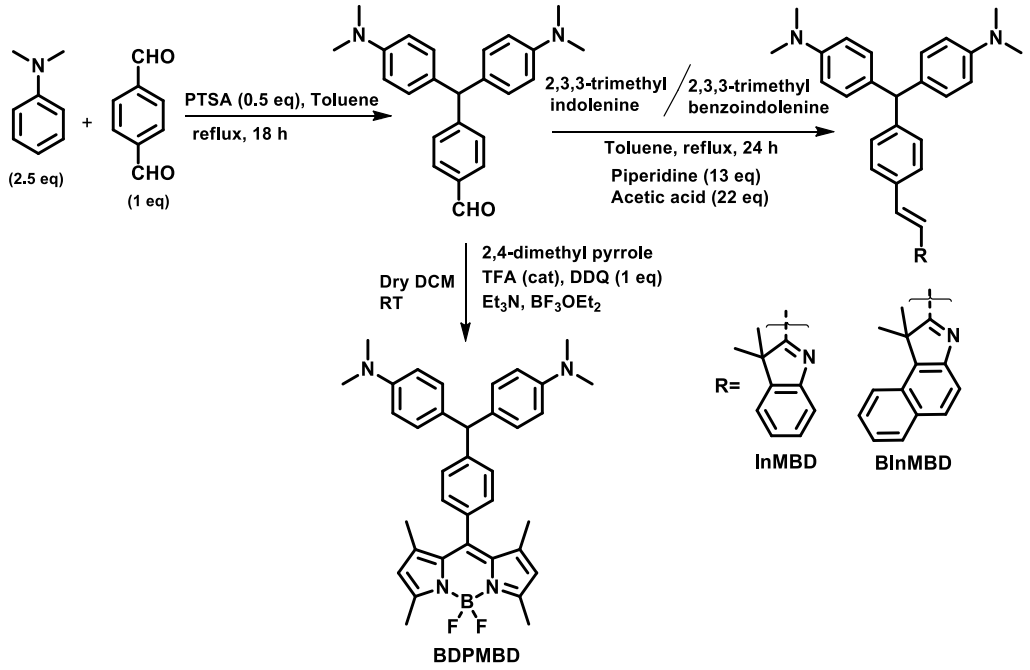

Scheme S1. Synthesis of leucomalachite green derivatives.

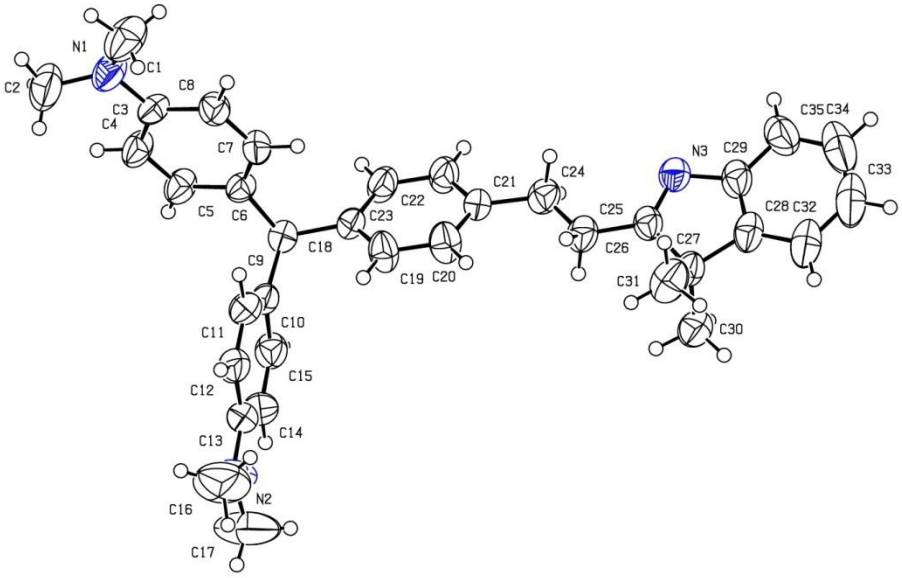

Fig. S1 ORTEP diagram of **InMBD**.

Table S1: X-ray crystallographic data and structural refinement details of **InMBD**

Identification code	**InMBD**
Empirical formula	C_{35} H_{37} N_3
Formula weight	499.67
Temperature	296(2) K
Wavelength	0.71073 A
Crystal system, space group	Monoclinic, P21/n
Unit cell dimensions	a = 13.777(3) A alpha = 90 deg b = 10.069(2) A beta = 91.861(12)deg c = 20.859(4) A gamma = 90 deg.
Volume	2892.2(11) A^3
Z, Calculated density	4, 1.148 Mg/m^3
Absorption coefficient	0.067 mm^{-1}
F(000)	1072
Crystal size	0.350 x 0.350 x 0.300 mm
Theta range for data collection	1.479 to 28.507 deg.
Limiting indices	-18<=h<=18, -13<=k<=9, -27<=l<=27
Reflections collected / unique	23022 / 7049 [R(int) = 0.0936]
Completeness to theta = 28.09	100.0 %
Absorption correction	Semi-empirical from equivalents
Max. and min. Transmission	0.980 and 0.977
Refinement method	Full-matrix least-squares on F^2
Data / restraints / parameters	7049 / 0 / 349
Goodness-of-fit on F^2	0.903
Final R indices [I>2sigma(I)]	R1 = 0.0677, wR2 = 0.1635
R indices (all data)	R1 = 0.2335, wR2 = 0.2625
Largest diff. peak and hole	0.242 and -0.234 $e.A^{-3}$

Detection of Fe^{3+}

The probe as well as Fe^{3+} stock solutions (0.01 M) were prepared in ethanol. 0-50 μM of Fe^{3+} was added to fixed concentration of the probes in 3 mL cuvette and stirred for 2 min. The change in absorbance at 630 nm were recorded for each of these solutions. The calibration plots were drawn by plotting the change in absorbance as a function of concentration. Emission intensity at 501 nm, 433 nm and 455 nm respectively were used for **BDPMBD**, **InMBD** and **BInMBD**. The change in emission

intensity as a function of concentration were used for drawing calibration plot. The concentrations of the probes used for the study is given below.

Colorimetric study: **BDPMBD** (10^{-5} M), **InMBD** (2×10^{-5} M), **BInMBD** (2×10^{-5} M)

Emission study: **BDPMBD** (10^{-6} M), **InMBD** (5×10^{-5} M), **BInMBD** (5×10^{-5} M)

Details of cyclic voltammetry experiments

The electrochemical studies of the compounds were performed in acetonitrile containing 0.1M tetrabutylammonium hexafluorophosphate as the supporting electrolyte at a scan rate of 100 mVs^{-1} under nitrogen atmosphere. The concentrations of the samples were maintained as 10^{-3} M. The electrodes used in the study were platinum (working), platinum wire (auxiliary) and Ag/AgCl (aq) (standard) electrodes.

Cell Imaging studies

Minimal essential medium (MEM), cell culture tested antibiotic and antimycotic solution, phosphate-buffered saline (PBS), tryptone, yeast extract, peptone, glucose, ammonium sulphate, dimethyl sulfoxide (DMSO), sodium chloride, and glycerol were obtained from HiMedia, Mumbai, India. Formaldehyde solution 37% was procured from MilliporeSigma (Burlington, Massachusetts, United States). Oleic acid and Hoechst 33342 was obtained from Sigma-Aldrich. Fetal Bovine Serum (FBS) was obtained from Invitrogen, CA, USA. Fluorescence microscopic images were taken using Nikon (Tokyo, Japan) ECLIPSE Ti-E inverted fluorescence microscope using Cool SNAP digital camera and processed using Image J (NIH, Bethesda). In cell imaging, the sections were examined with Leica, TCS SP8 confocal microscope.

Organisms used in the biological study and growth conditions

Human cervical cancer cells (HeLa) were obtained from National Centre for Cell Science (NCCS), Pune, India. HeLa cells were grown in MEM supplemented with 10% (v/v) FBS, sodium bicarbonate and 1% antibiotic-antimycotic solution containing 100 units of penicillin, 100 µg of streptomycin, and 0.25 µg of amphotericin B per mL. Cells were maintained in 25 cm^2 tissue culture flasks at 37 °C in a humidified atmosphere of 5% CO_2 and 95% air.

Laboratory strain of Baker's yeast *Saccharomyces cerevisiae* was grown in aerobic conditions in a defined YPD medium supplemented with 1% yeast extract, 2% peptone, and 2% glucose. To enhance the lipid production profile inside the yeast cells, the cells were separately grown in a modified medium containing 2% peptone, ammonium sulfate (3 g/L) as the sole nitrogen source, oleic acid (50 µM) and glycerol (100 g/L) as a sole carbon source. *Escherichia coli* (EC) (BL21 (DE3)) and *Bacillus subtilis* 168 (BS) were grown in aerobic conditions in a liquid medium supplemented with yeast extract (0.5%), tryptone (1.5%), and NaCl (1%)

Localization studies of the compounds in HeLa cells using fluorescence microscopy

To study the localization of compounds **InMBD**, **BInMBD**, and **BDPMBD**, HeLa cells at a density of 0.5×10^5 cells/mL were seeded on poly-L-lysine coated glass cover slips in 24-well tissue culture plates. Next day, the cells were incubated with each of these compounds (50 µM) separately for 24 h. The cells were then washed twice with 1xPBS to remove the excess un-internalized compounds. Further, the cells were fixed with 3.7% formaldehyde and were subsequently stained with nuclear stain Hoechst 33342 (1.5 µg/mL). [The localization in live HeLa cells was studied by incubating the HeLa cells with compounds **BDPMBD** (100 µM), **BInMBD** (100 µM), and **InMBD** (100 µM).] The cover slips containing fixed & live cells were mounted on clean glass slides and the cells were observed using an inverted fluorescence microscope.

Confocal imaging in live HeLa and DLD cells

The localization of the compounds in the live HeLa cells and DLD cells (0.5×10^5 cell/mL) were studied by incubating the cells with **BDPMBD** (100 µM). After 18 h of incubation, the cells were subsequently stained with Nile red (0.3 µM). Then the cells were washed twice with 1xPBS to remove the excess un-internalized compounds. The coverslips containing the live cells were then mounted on clean glass slides and the cells were observed under a confocal fluorescence microscope using different emission filters.

pH sensing studies of InMBD, BInMBD, and BDPMBD in Baker's yeast, *Escherichia coli,* and *Bacillus subtilis* cells.

Briefly, yeast, *E. coli* and *B. subtilis* cells were separately incubated with a fixed concentration (100 µM) of the compounds for 4 h. The cells were then harvested and washed twice with 1xPBS. Further, the cells were fixed with 4% formaldehyde solution for 30 min at RT. After this, the cell suspension was centrifuged and the supernatant containing 4% formaldehyde solution was decanted. The yeast and bacterial cells were then incubated with buffer solutions ranging from pH 1-9 for 1 h at room temperature to equilibrate the intracellular pH with the pH of the buffers.

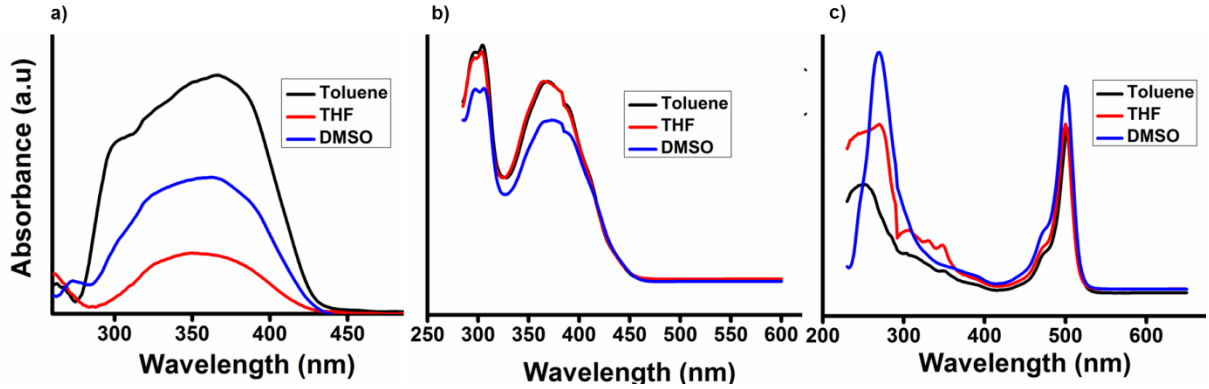

Fig. S2 Absorption spectra of 5 × 10^{-5} M solution of a) **InMBD**, b) **BInMBD**, & c) **BDPMBD** in different solvents.

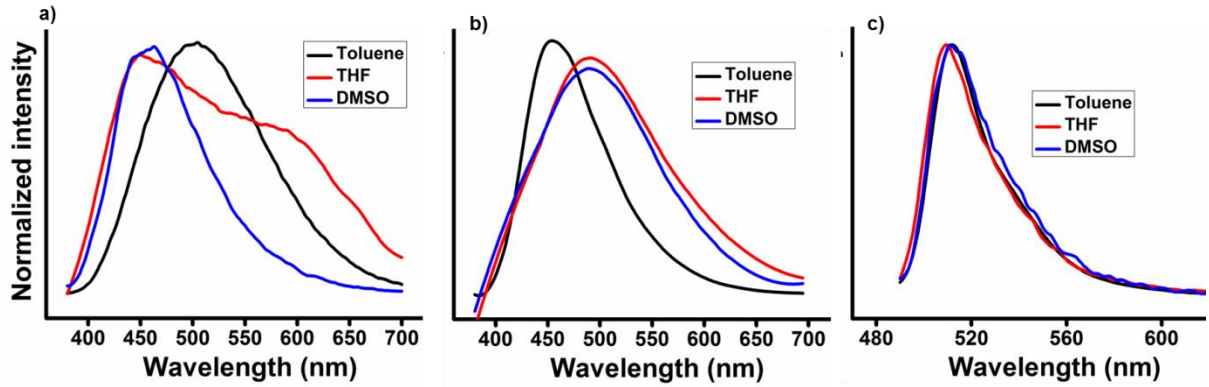

Fig. S3 Emission spectra of 5 × 10^{-5} M solution of a) **InMBD**, b) **BInMBD**, & c) **BDPMBD** in different solvents.

Table S2. Spectral data of **InMBD** in different solvents.

Solvent	**Absorbance (nm)**	**Emission (nm)**	**Stokes shift (nm)**	**Quantum yield***	**Quantum yield at pH=2***
Toluene	365	502	137	0.223	
THF	357	450	93	0.041	0.090
Ethyl acetate	354	507	153	0.043	
Acetonitrile	354	450	96	0.034	0.078
DMF	357	444	87	0.053	
DMSO	362	463	101	0.032	0.069

*Quantum yield measurements were done using quinine sulphate as the standard.

Table S3. Spectral data of **BInMBD** in different solvents.

Solvent	**Absorbance (nm)**	**Emission (nm)**	**Stokes shift (nm)**	**Quantum yield***	**Quantum yield at pH=2***
Toluene	367	455	88	0.154	
THF	367	490	123	0.073	0.168
Ethyl acetate	364	492	128	0.057	
Acetonitrile	362	493	131	0.037	0.124
DMF	366	487	121	0.082	
DMSO	373	490	117	0.040	0.160

*Quantum yield measurements were done using quinine sulphate as the standard.

Table S4. Spectral data of **BDPMBD** in different solvents.

Solvent	**Absorbance (nm)**	**Emission (nm)**	**Stokes shift (nm)**	**Quantum yield***	**Quantum yield at pH=2***
Toluene	502	512	10	0.58	
THF	500	510	10	0.202	
Ethyl acetate	498	507	9	0.311	
Acetonitrile	496	507	11	0.136	
DMF	500	510	10	0.103	
DMSO	500	511	11	0.092	0.332

*Quantum yield measurements were done using quinine sulphate as the standard.

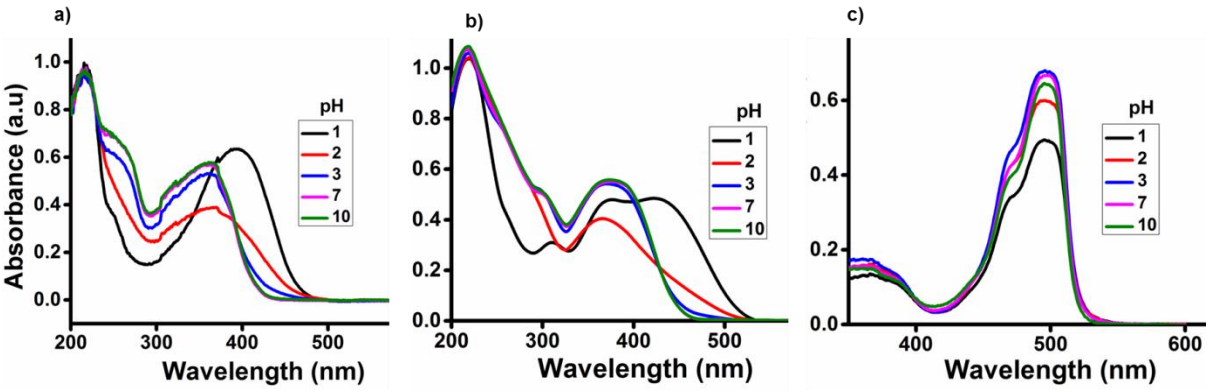

Fig. S4 pH-dependent absorption spectra of 5 × 10^{-5} M solution of a) **InMBD** b) **BInMBD** & c) **BDPMBD** in acetonitrile (MeCN):BR buffer (1:1).

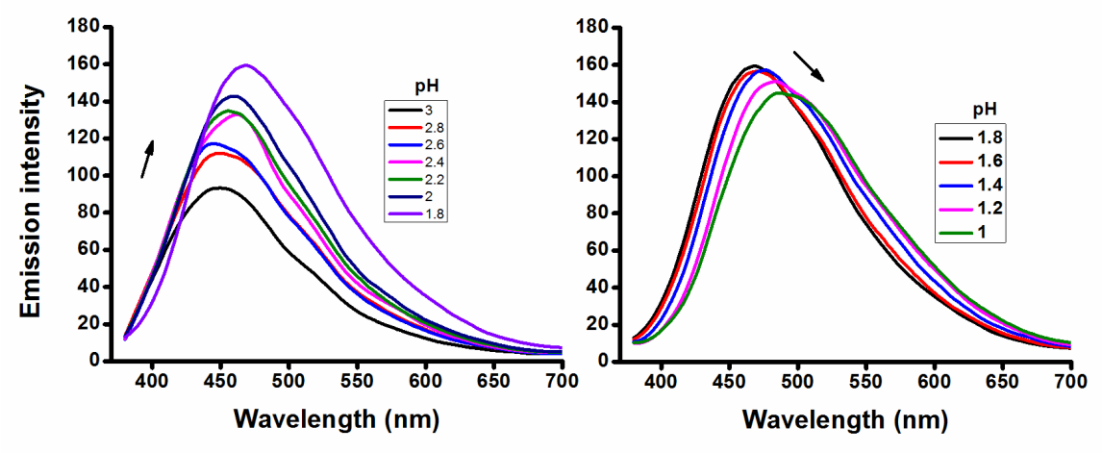

Fig. S5 pH-dependent emission spectra of 5×10^{-5} M solution of **InMBD** (λ_{ex} = 360 nm).

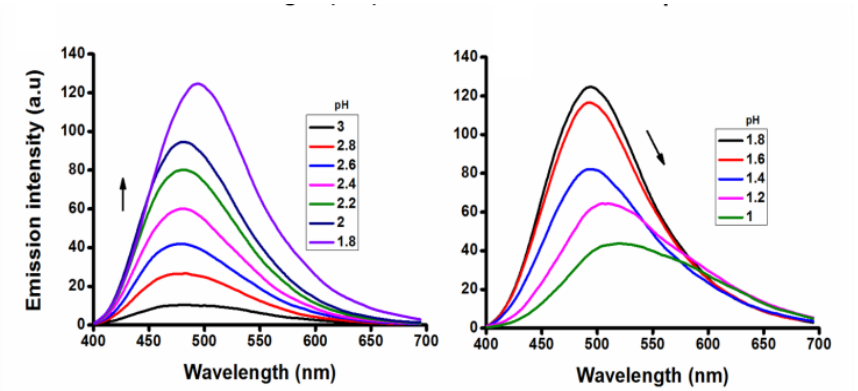

Fig. S6 pH-dependent emission spectra of 5×10^{-5} M solution of **BInMBD** (λ_{ex} = 360 nm).

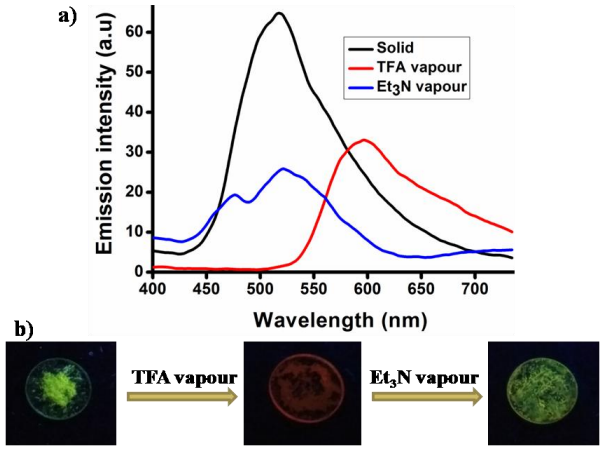

Fig. S7 a) Emission spectra of solid **BInMBD** on exposure to acid and base vapours b) photograph under UV light of 365 nm.

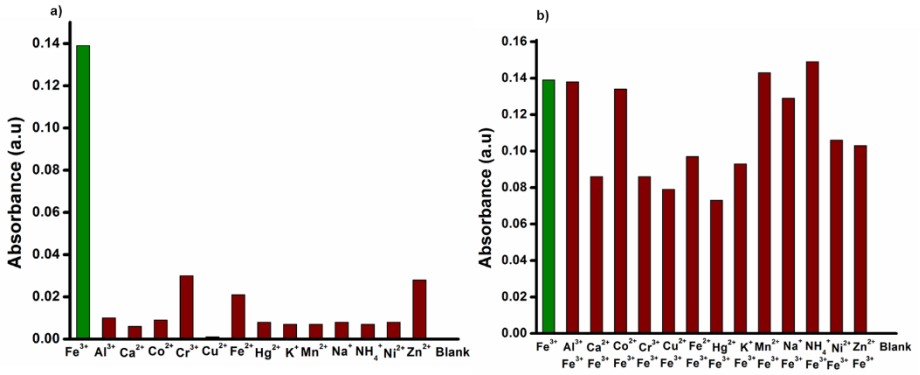

Fig. S8 a) The selectivity and b) competitive selectivity of **InMBD** (20 µM) towards Fe^{3+} (absorbance at 630 nm; Fe^{3+} (5eq), Cr^{3+}, Cu^{2+}, Fe^{2+} (each 10 eq) and other metal ions (100 eq) were used).

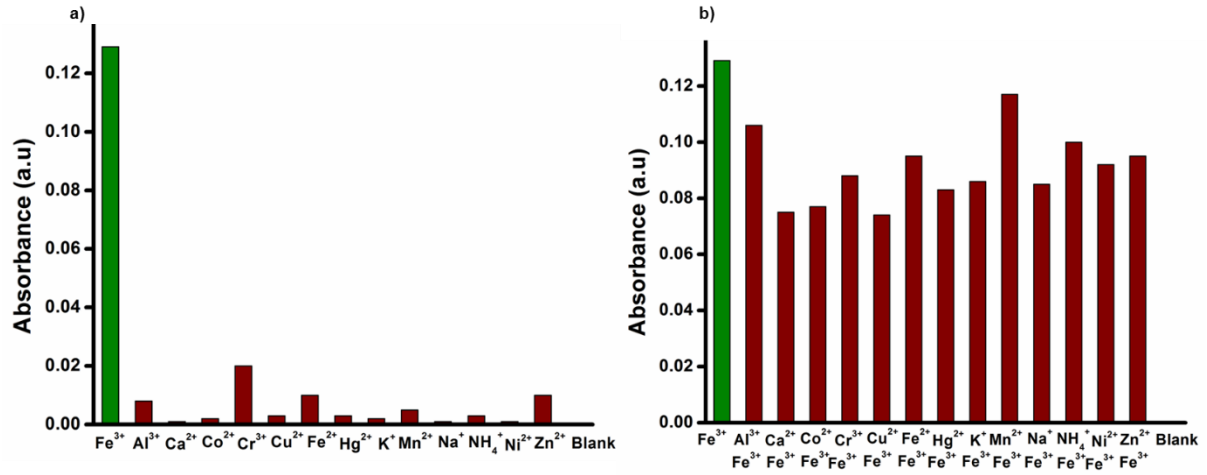

Fig. S9 a) The selectivity and b) competitive selectivity of **BInMBD** (20 µM) towards Fe^{3+} (absorbance at 630 nm; Fe^{3+} (5eq), Cr^{3+}, Cu^{2+}, Fe^{2+} (each 10 eq) and other metal ions (100 eq) were used).

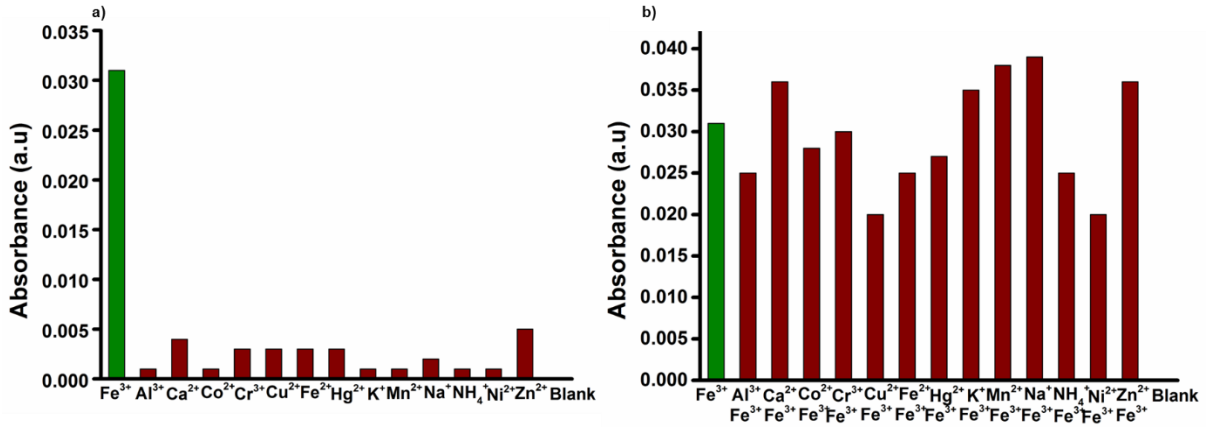

Fig. S10 a) The selectivity and b) competitive selectivity of **BDPMBD** (10 µM) towards Fe^{3+} (absorbance at 630 nm; Fe^{3+} (5eq), Cr^{3+}, Cu^{2+}, Fe^{2+} (each 10 eq) and other metal ions (100 eq) were used).

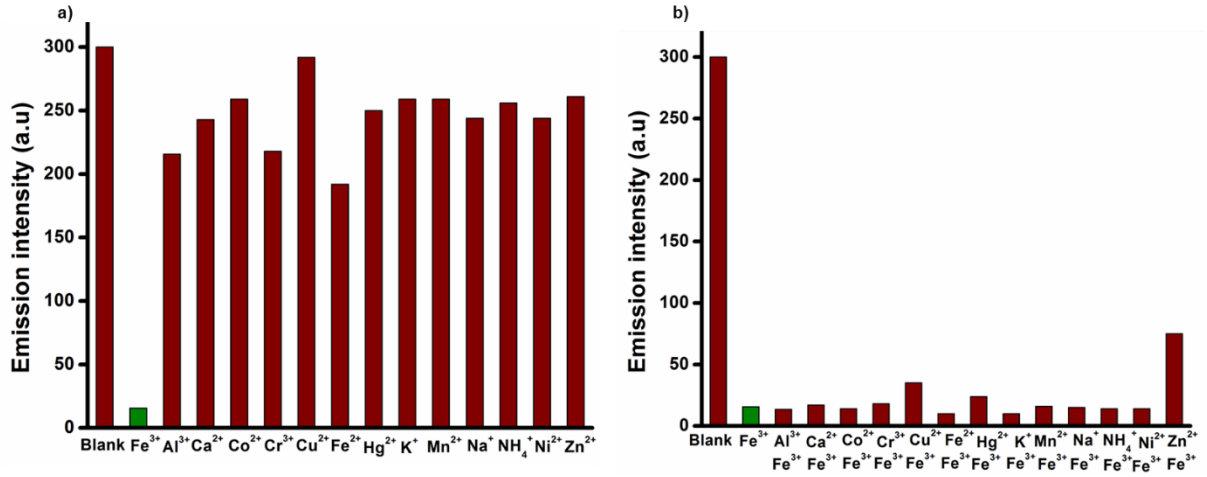

Fig. S11 a) The selectivity and b) competitive selectivity of **InMBD** (20 µM) towards Fe^{3+} (emission at 417 nm; Fe^{3+} (5eq), Cr^{3+}, Cu^{2+}, Fe^{2+} (each 10 eq) and other metal ions (100 eq) were used).

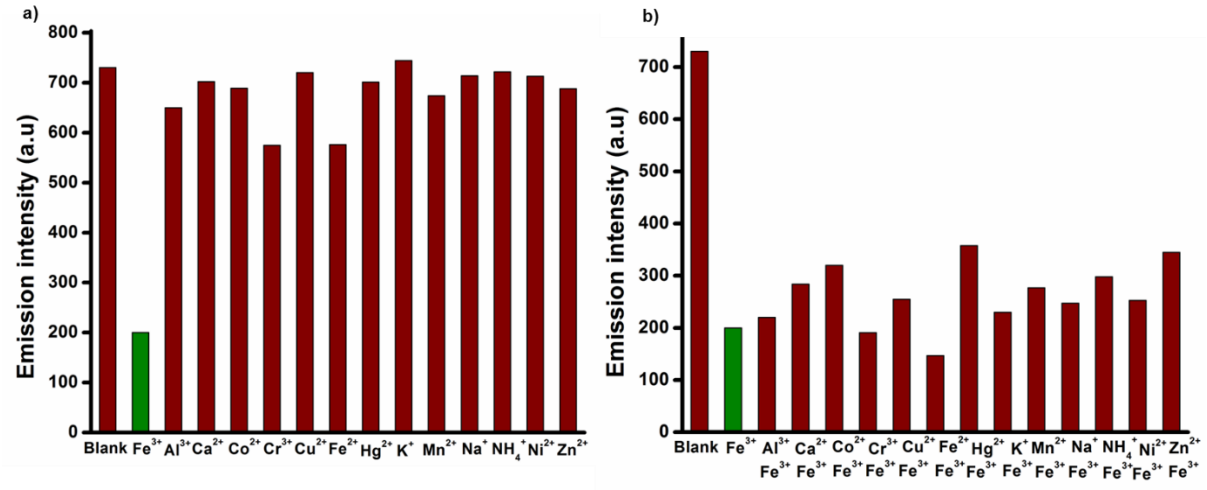

Fig. S12 a) The selectivity and b) competitive selectivity of **BInMBD** (20 µM) towards Fe^{3+} (emission at 444 nm; Fe^{3+} (5eq), Cr^{3+}, Cu^{2+}, Fe^{2+} (each 10 eq) and other metal ions (100 eq) were used).

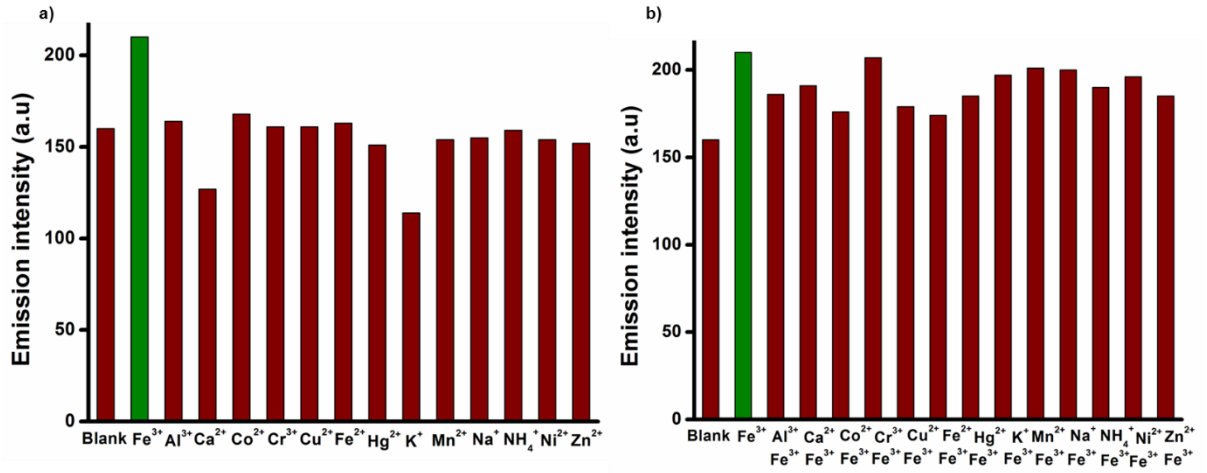

Fig. S13 a) The selectivity and b) competitive selectivity of **BDPMBD** (10 µM) towards Fe^{3+} (emission at 498 nm; Fe^{3+} (5eq), Cr^{3+}, Cu^{2+}, Fe^{2+} (each 10 eq) and other metal ions (100 eq) were used).

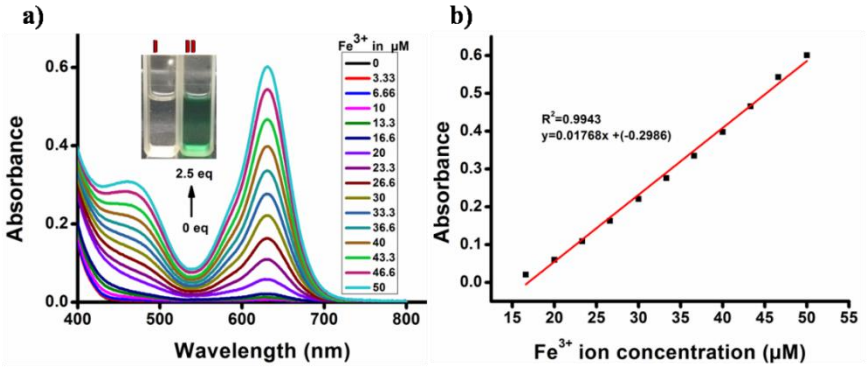

Fig. S14 a) Absorption spectra of 2×10^{-5} M solution of **InMBD** in the presence of varying amounts of Fe^{3+}; Inset: I-before & II- after addition of Fe^{3+} & b) the corresponding calibration plot.

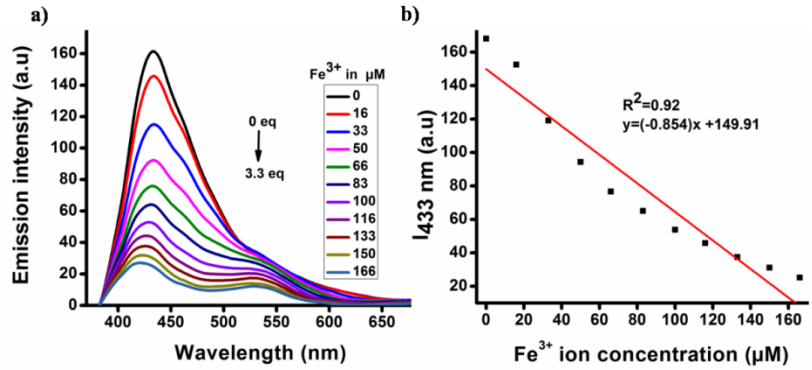

Fig. S15 a) Emission spectra of 5×10^{-5} M solution of **InMBD** in presence of varying amounts of Fe^{3+} & b) the corresponding calibration plot.

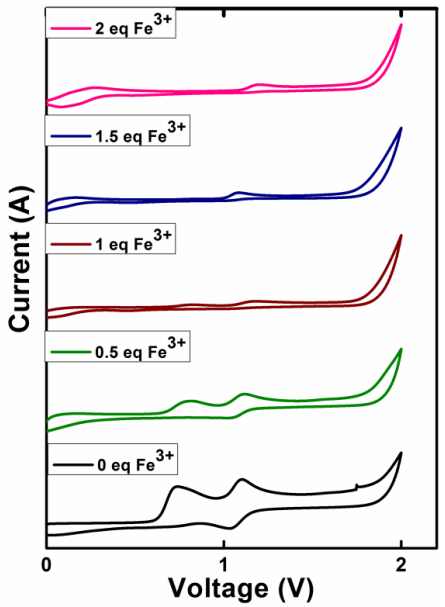

Fig. S16 Cyclic voltammogram of **InMBD** with varying concentration of Fe^{3+}. Scan rate = 100 mV/s, V vs $Ag/Ag^{+}_{(aq)}$.

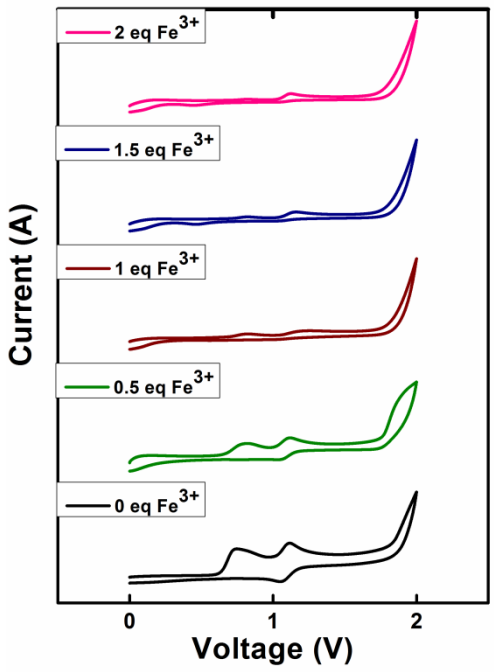

Fig. S17 Cyclic voltammogram of **BInMBD** with varying concentration of Fe^{3+}. Scan rate = 100 mV/s, V vs $Ag/Ag^{+}_{(aq)}$.

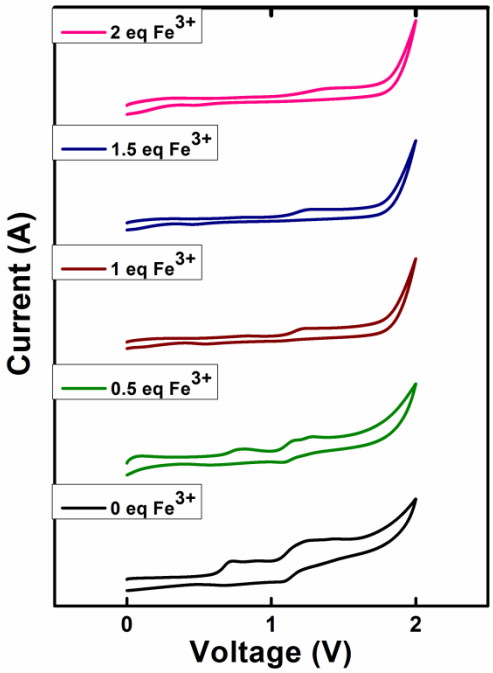

Fig. S18 Cyclic voltammogram of **BDPMBD** with varying concentration of Fe^{3+}. Scan rate = 100 mV/s, V vs $Ag/Ag^{+}_{(aq)}$.

Determination of cytotoxicity using Sulforhodamine B (SRB) assay

The effect of the compounds **BDPMBD**, **BInMBD**, and **InMBD** on the proliferation of HeLa cells was determined by performing the standard SRB assay. Briefly, HeLa cells were seeded in the 96-well plates at a seeding density of 0.5×10^5 cells/mL. After 24 h, the medium of the cells was changed and the fresh medium containing different concentrations (0-300 µM) of **BDPMBD**, **BInMBD**, or **InMBD** was added. The cells were then allowed to grown in the presence of the compounds for one cell cycle. After 24 h, the cells were fixed with 10% trichloroacetic acid and were subsequently stained with 0.4% SRB for 1 h. The cell-bound dye was then extracted with 10 mM Tris base (pH 10.5) and the optical density at 560 nm was determined using 96-well micro plate reader. The percentage inhibition of cell proliferation was determined as described previously.

The compounds BDPMBD, BInMBD, and InMBD induced minimal toxicity in HeLa cells

The effect of the compounds **BDPMBD**, **InMBD**, and **BInMBD** on the proliferation of HeLa cells was determined using SRB assay. It is evident from Fig. S19 A that the compound **BDPMBD** inhibited proliferation of HeLa cells in a concentration dependent manner with an IC_{50} value of 270 µM. Increasing concentrations of the compound **BDPMBD** such as 40, 80, 100, 150, 200, and 300 µM inhibited the proliferation of HeLa cells by 2, 10, 15, 24, 36, and 56% respectively. The compound **BInMBD** inhibited the proliferation of HeLa cells with an IC_{50} value of 240 µM. Increasing concentrations of the compound **BInMBD** such as 40, 80, 100, 150, 200, and 300 µM inhibited the proliferation of HeLa cells by 13, 24, 29, 33, 45, and 55% respectively (Fig. S19 B). The compound **InMBD** inhibited the proliferation of HeLa cells with an IC_{50} value of 215 µM. Increasing concentrations of the compound **InMBD** such as 40, 80, 100, 150, 200, and 300 µM inhibited the proliferation of HeLa cells by 19, 21, 27, 36, 46, and 69% respectively (Fig. S19 C). Our results indicate that the compound **InMBD** (IC_{50} value of 215 µM) exhibited better anti-proliferative potency as compared to **BDPMBD** and **BInMBD** in the HeLa cells. Also the data indicates all the three compounds exhibited relatively higher IC_{50} values indicating that the exposure to these compounds caused minimal toxicity in the HeLa cells.

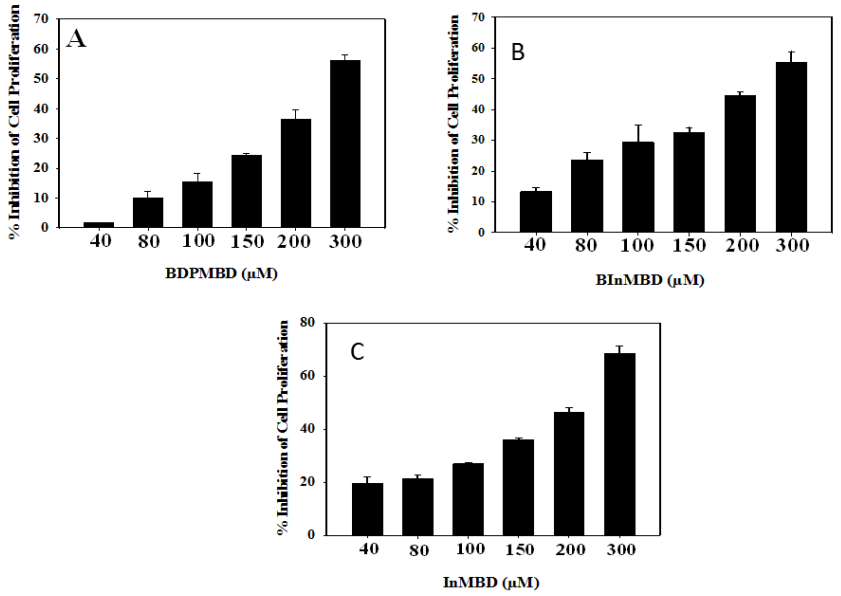

Fig. S19 HeLa cells (0.5×10^5 cells/mL) were incubated in the absence and presence of the compounds A) **BDPMBD** B) **BInMBD** C) **InMBD** for 24 h and the percentage inhibition of cell proliferation was determined by using SRB assay. The experiment was performed three times. Error bars represent ± SD.

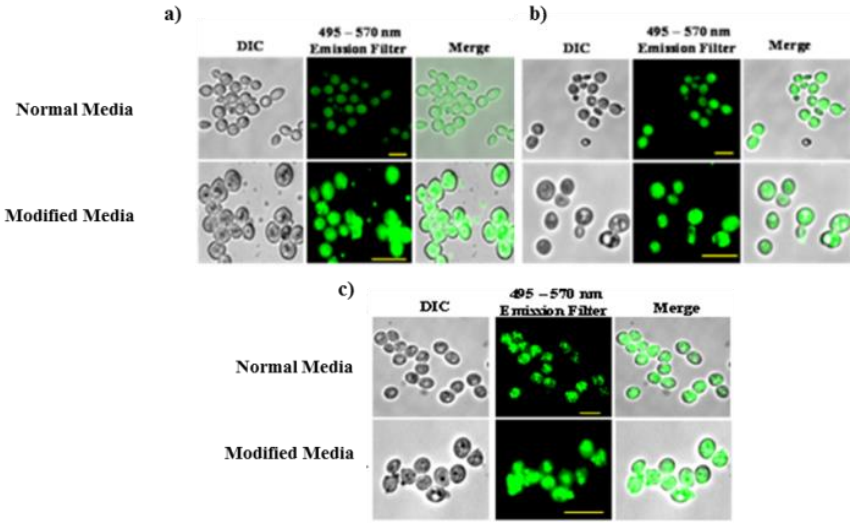

Fig. S20 Cellular localization of compounds a) **InMBD** b) **BInMBD,** & c) **BDPMBD** in yeast cells. Scale bar =10 µm.

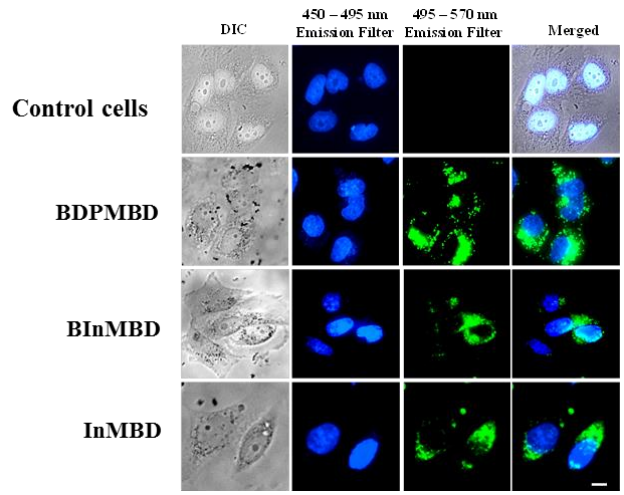

Fig. S21 Cellular localization of the compounds **BDPMBD, BInMBD**, and **InMBD** in fixed HeLa cells. Scale bar =10 µm.

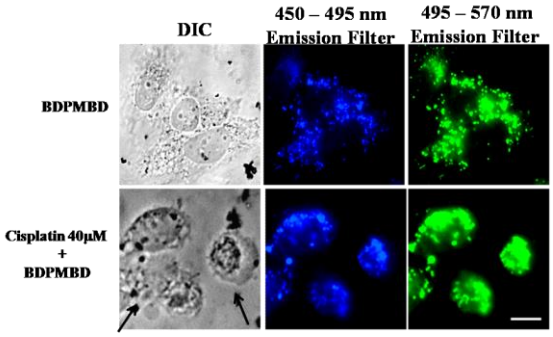

Fig. S22 Detection of apoptotic cells using **BDPMBD**. Scale bar =10 µm.

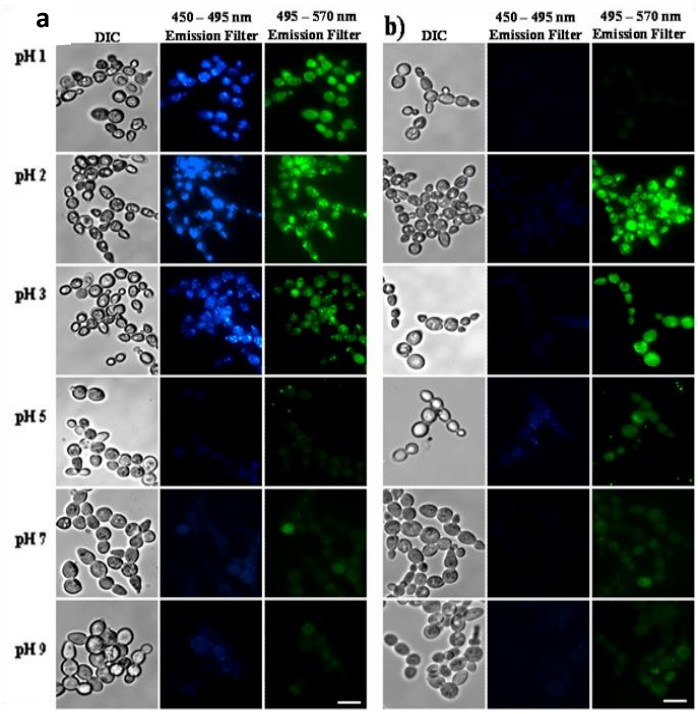

Fig. S23 pH-dependent fluorescence switching of compounds a) **BInMBD** and b) **InMBD** in *S. cerevisiae* cells. Scale bar =10 µm.

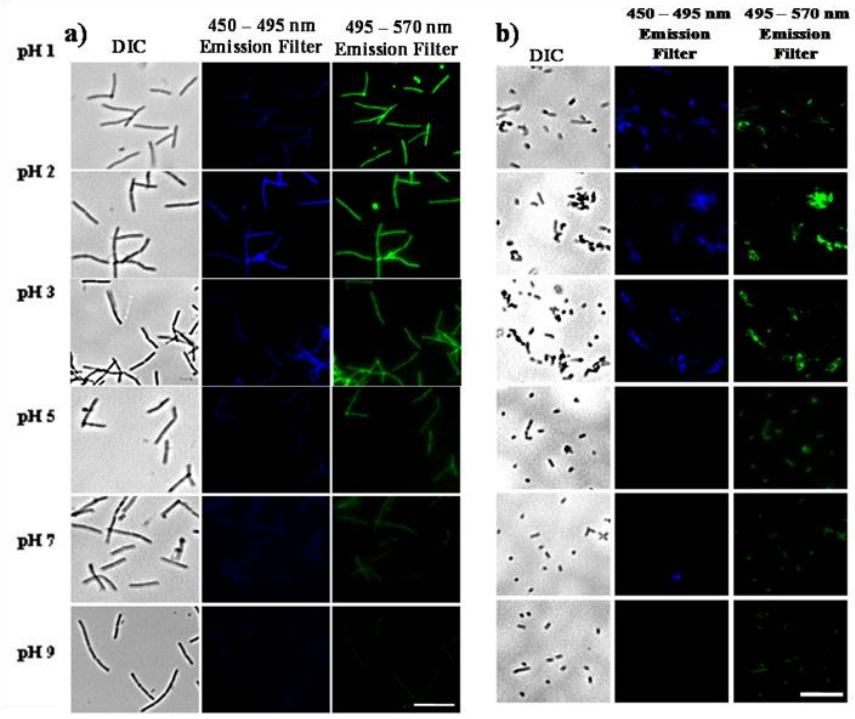

Fig. S24 pH-dependent fluorescence switching of **BInMBD** in a) gram-positive bacteria *Bacillus subtilis* & b) gram-negative bacteria *E. Coli*. Scale bar = 5 µm.

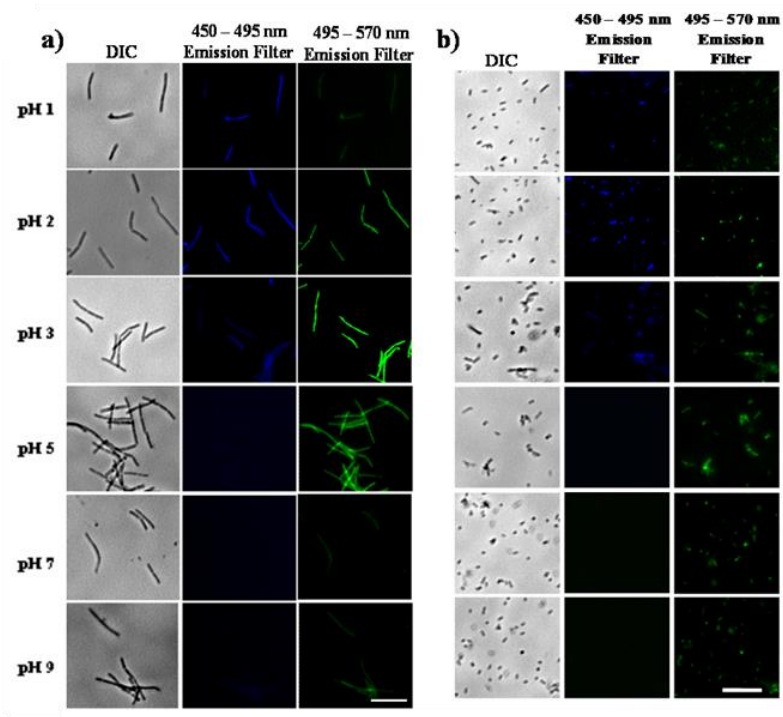

Figure S25. pH-dependent fluorescence switching of **InMBD,** in a) gram-positive bacteria *Bacillus subtilis* & b) gram-negative bacteria *E. Coli*. Scale bar =5 µm.

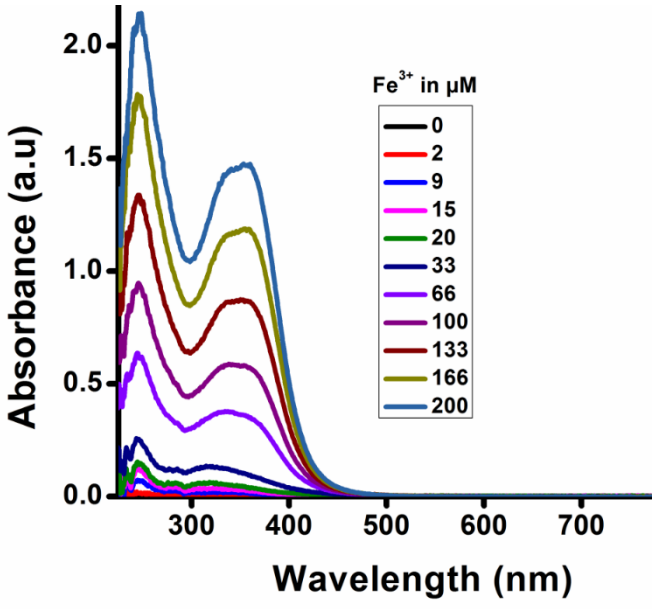

Figure S26. Absorption spectra of Fe^{3+} in ethanol at a concentration range of 0-200 µM.

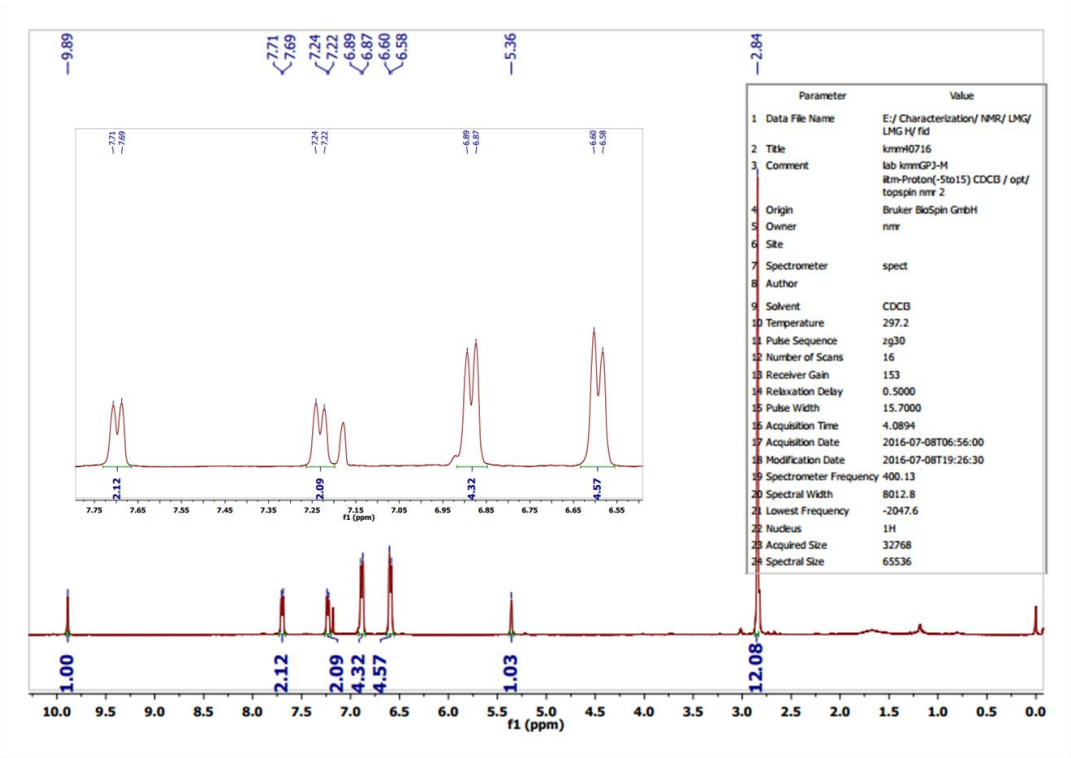

Fig. S27 ^{1}H NMR spectrum of **LMG-CHO** (400 MHz, $CDCl_3$).

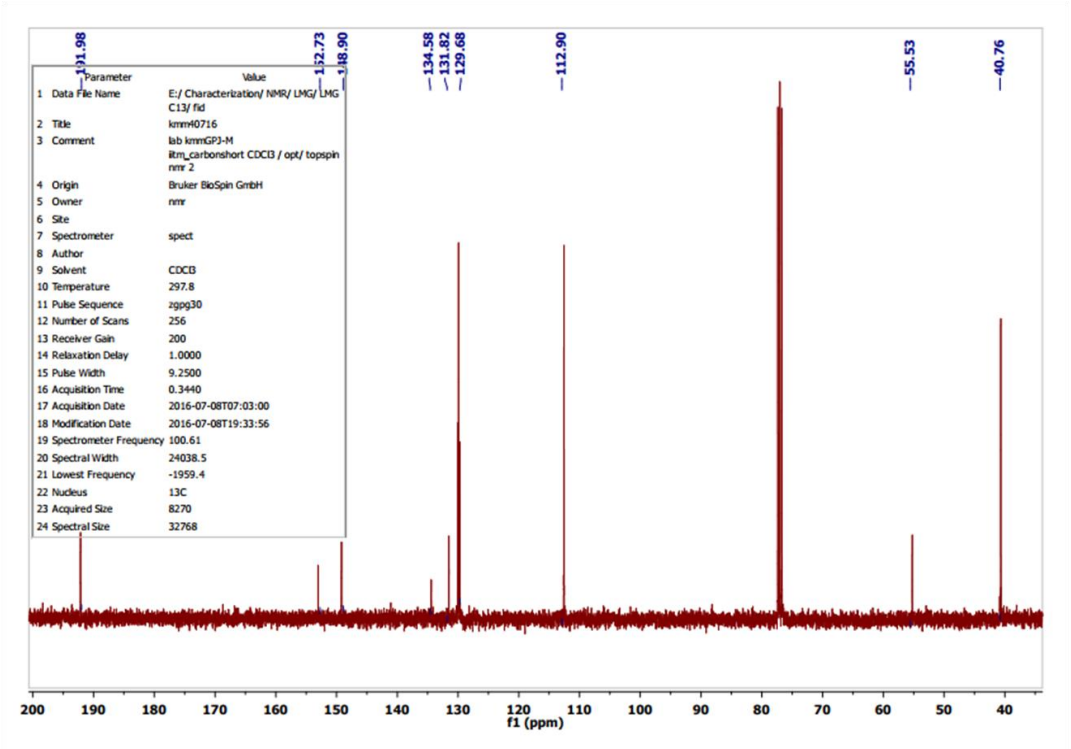

Fig. S28 ^{13}C NMR spectrum of **LMG-CHO** (100 MHz, $CDCl_3$).

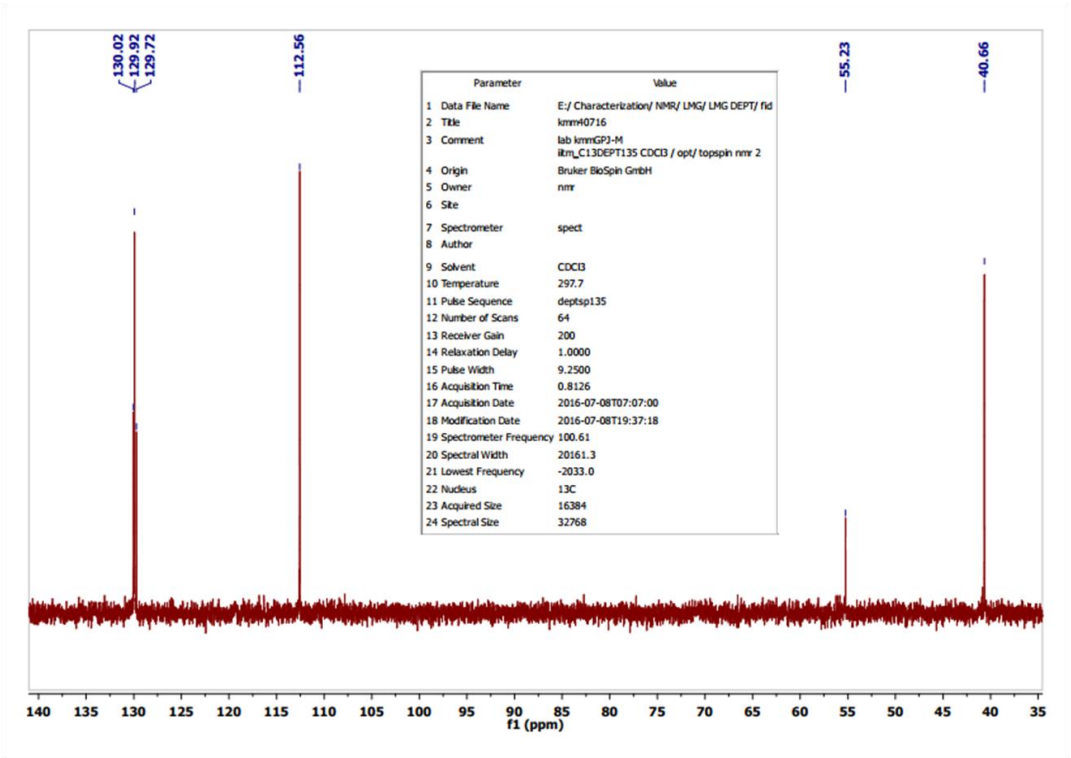

Fig. S29 DEPT-135 of **LMG-CHO** (100 MHz, $CDCl_3$).

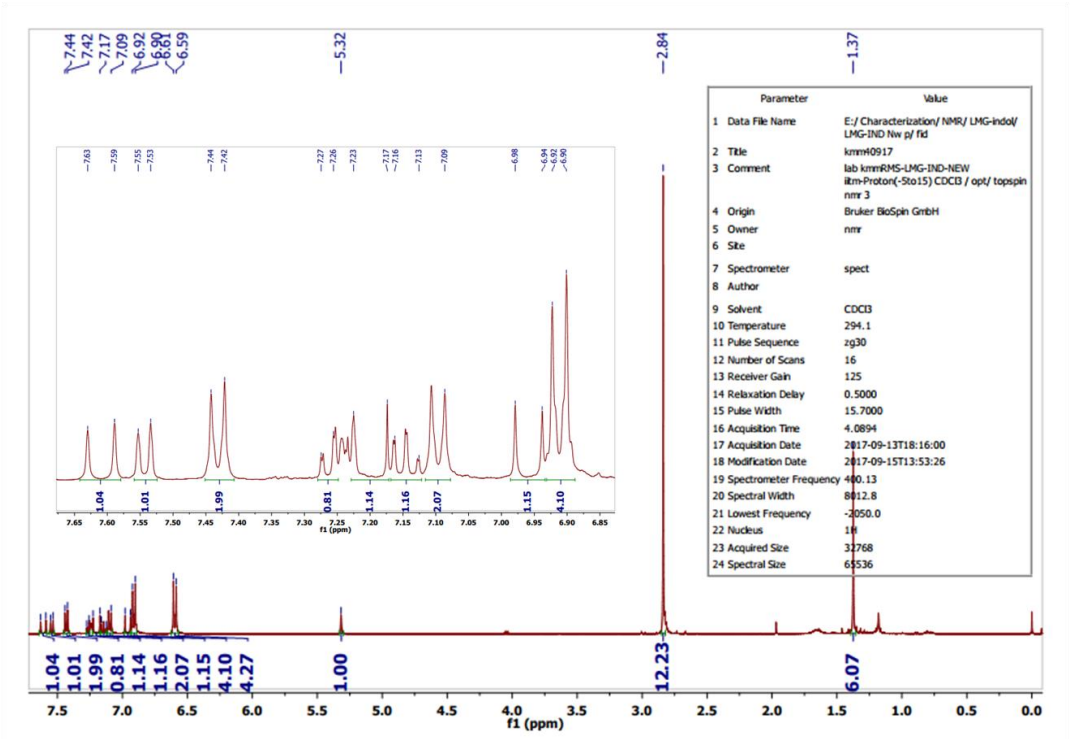

Fig. S30 ^{1}H NMR spectrum of **InMBD** (400 MHz, $CDCl_3$).

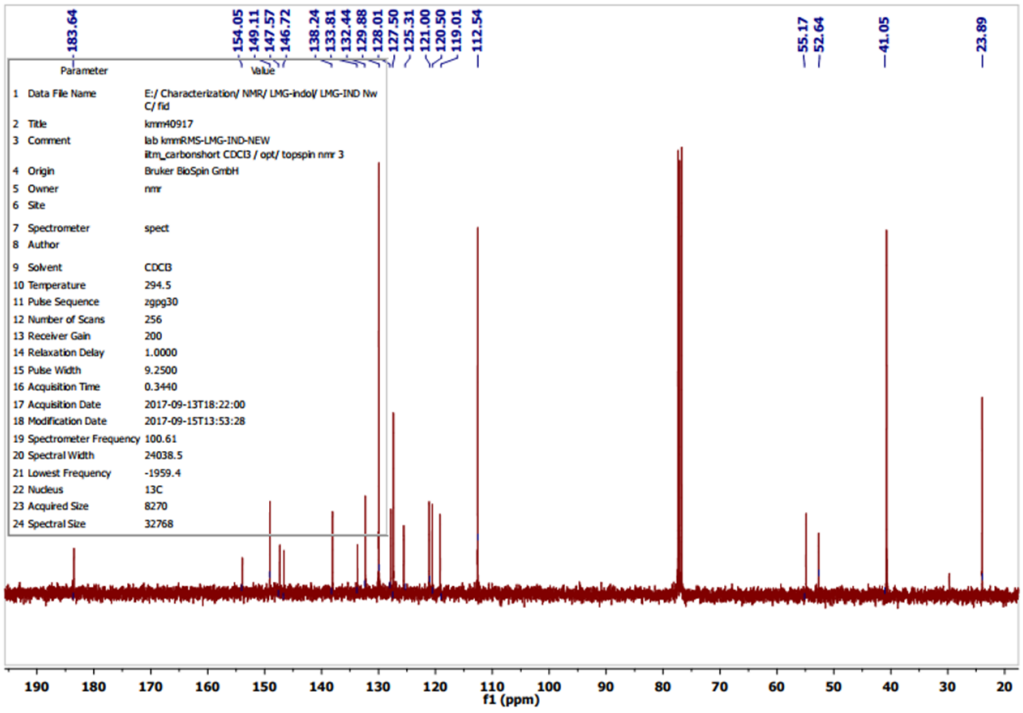

Fig. S31 ^{13}C NMR spectrum of **InMBD** (100 MHz, $CDCl_3$).

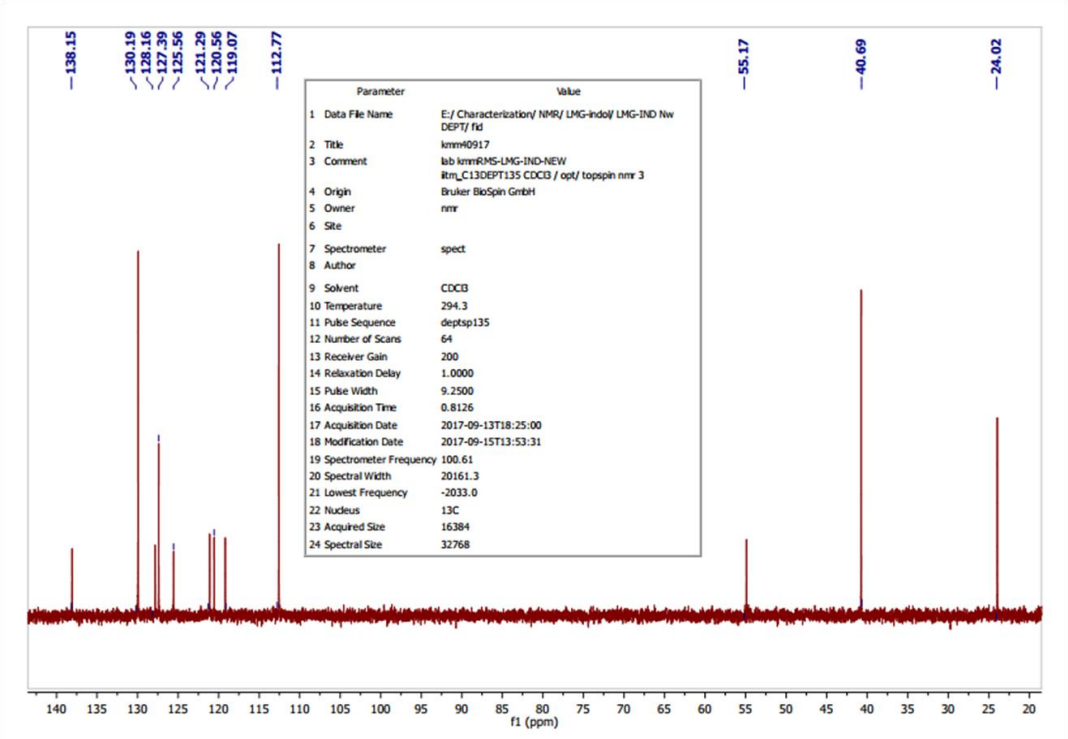

Fig. S32 DEPT-135 of **InMBD** (100 MHz, $CDCl_3$).

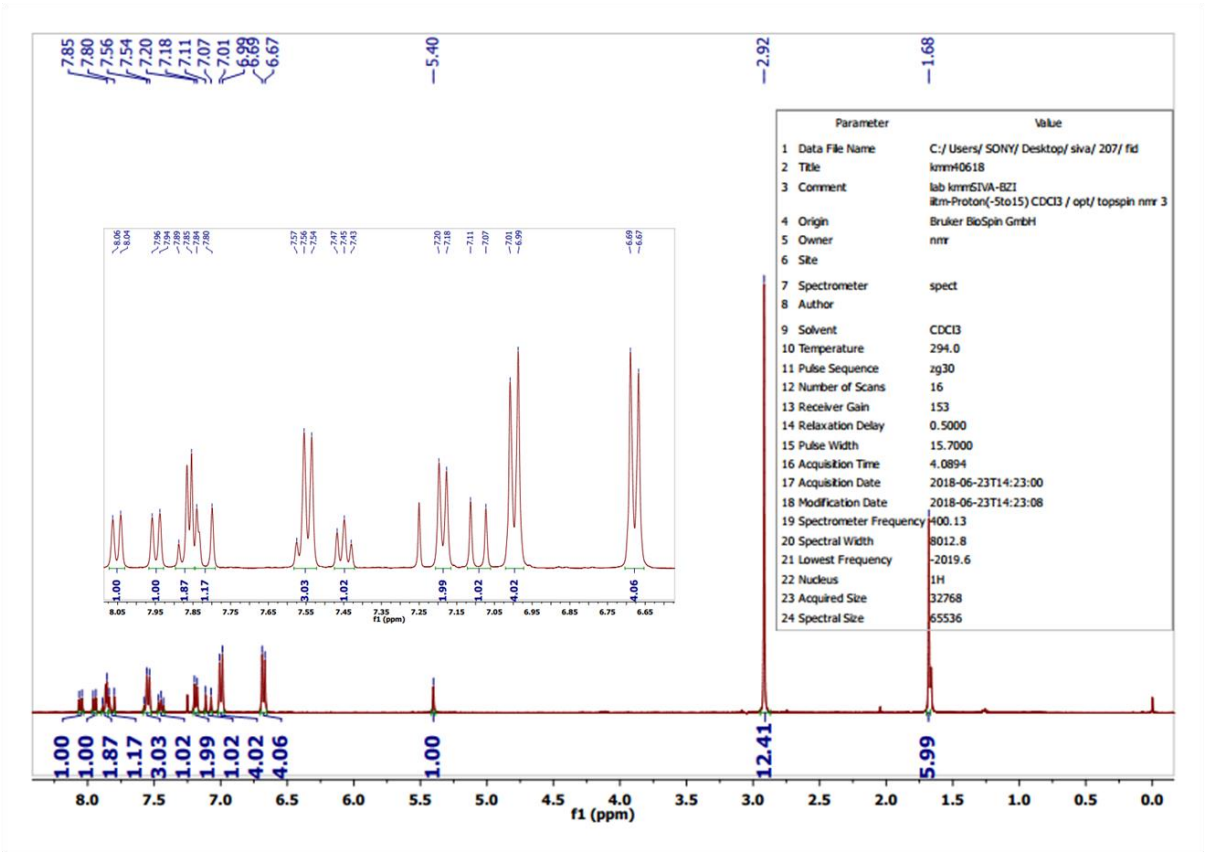

Fig. S33 ^{1}H NMR spectrum of **BInMBD** (400 MHz, $CDCl_3$).

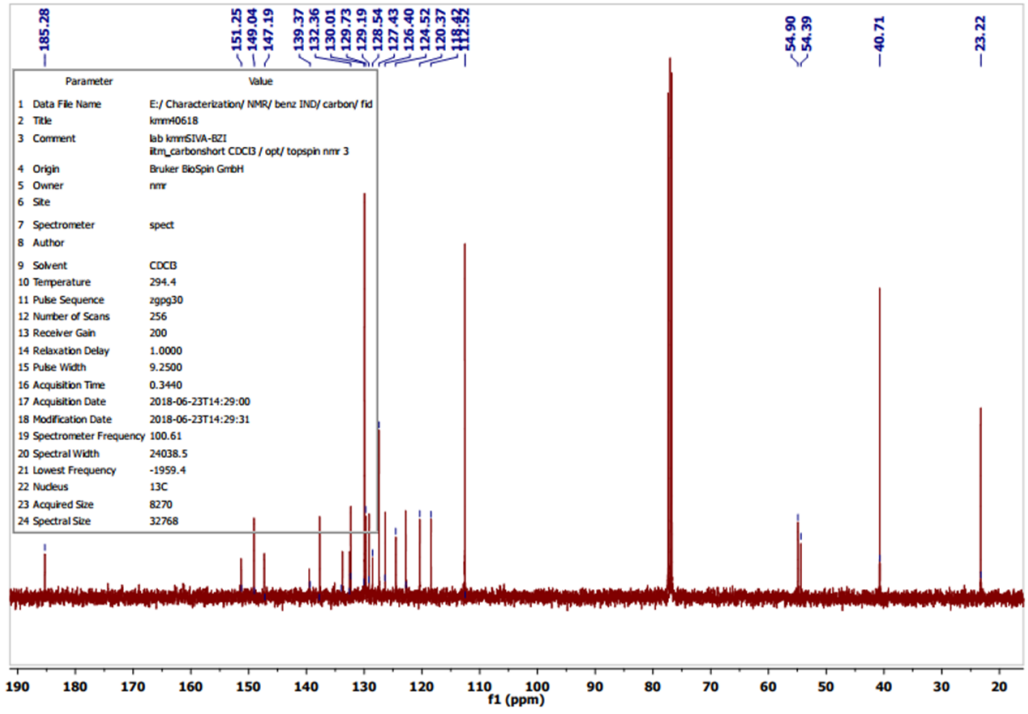

Fig. S34 ^{13}C NMR spectrum of **BInMBD** (100 MHz, $CDCl_3$).

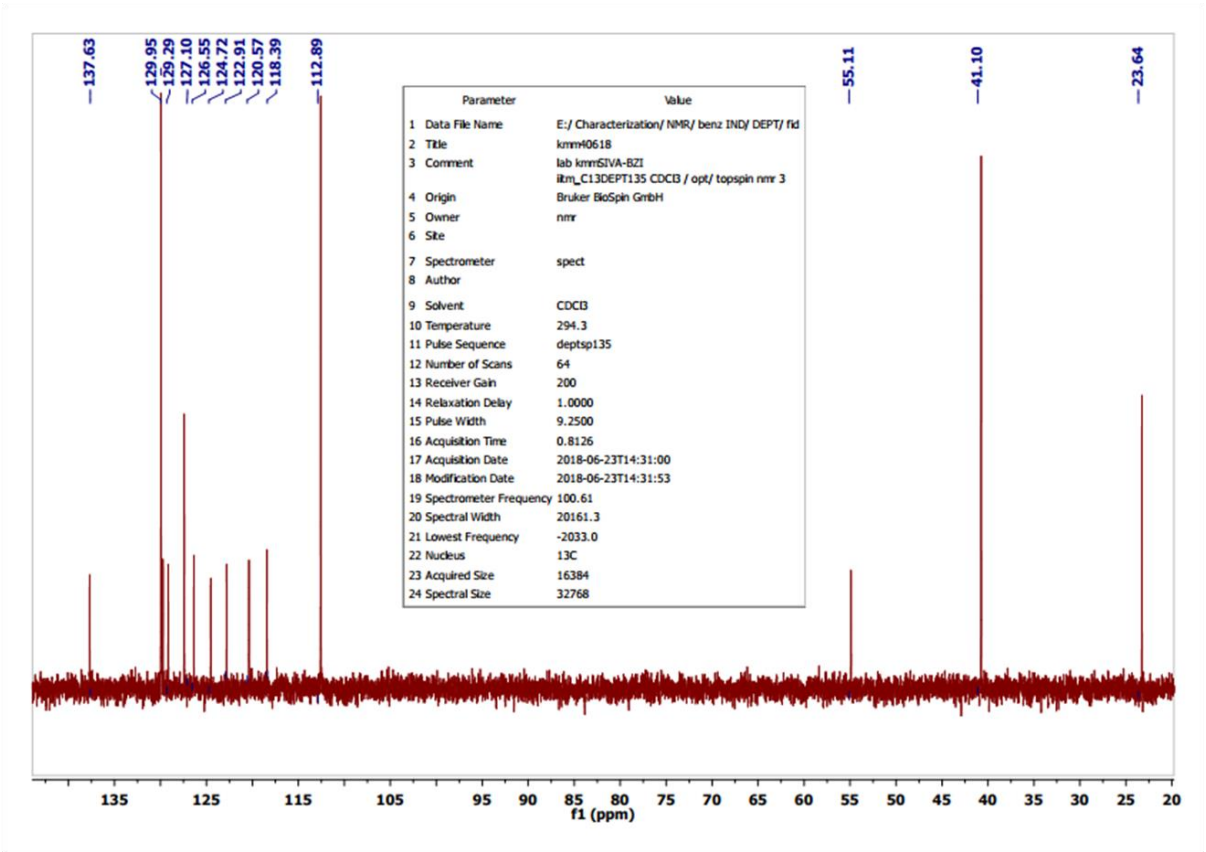

Fig. S35 DEPT-135 of **BInMBD** (100MHz, $CDCl_3$).

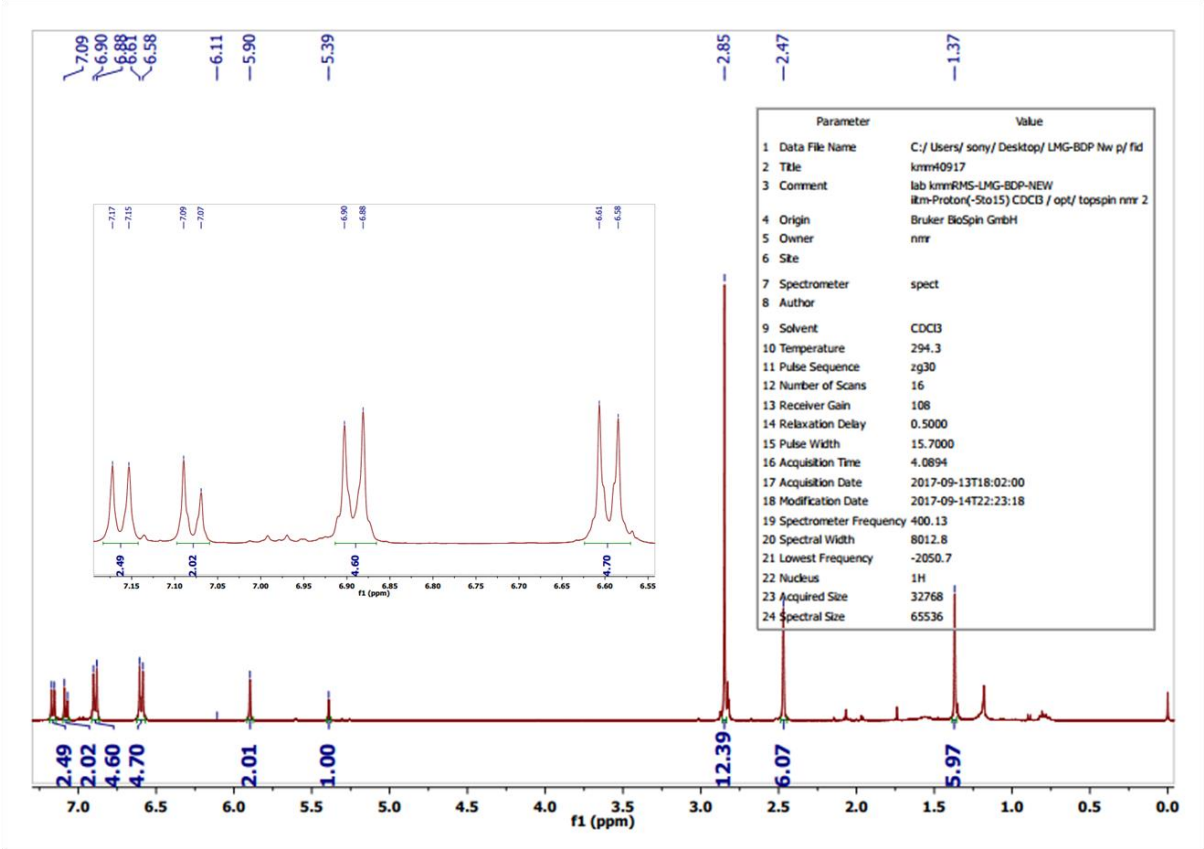

Fig. S36 ^{1}H NMR spectrum of **BDPMBD** (400 MHz, $CDCl_3$).

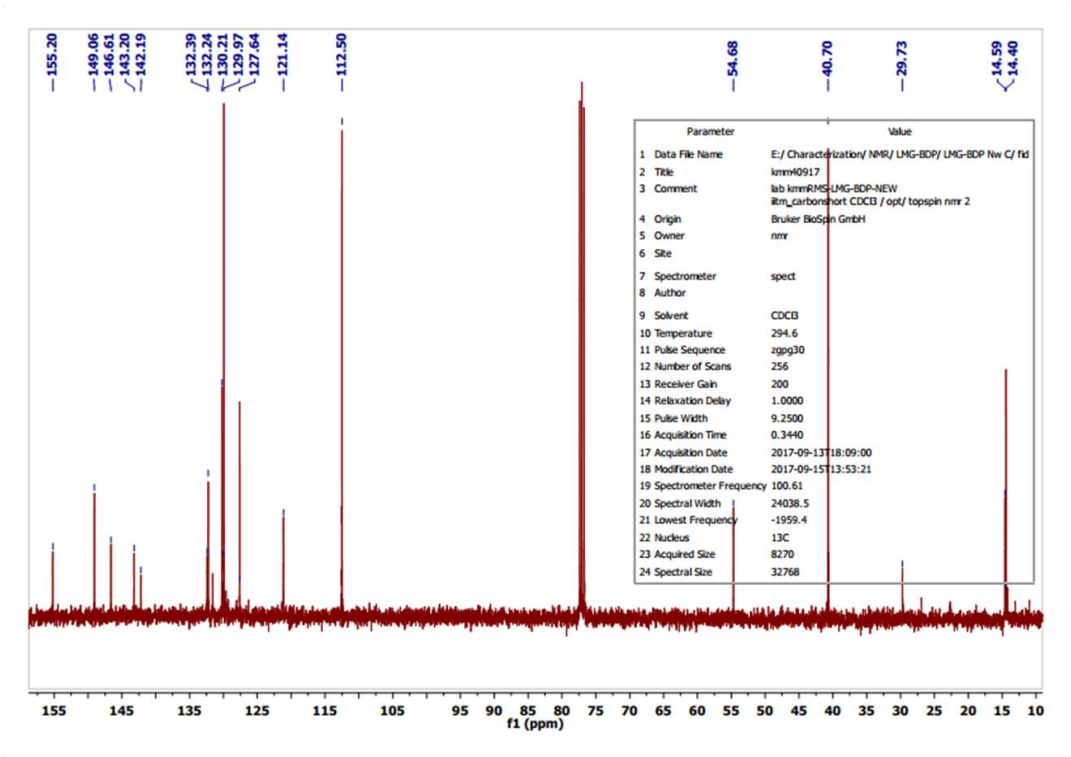

Fig. S37 ^{13}C NMR spectrum of **BDPMBD** (100 MHz, $CDCl_3$).

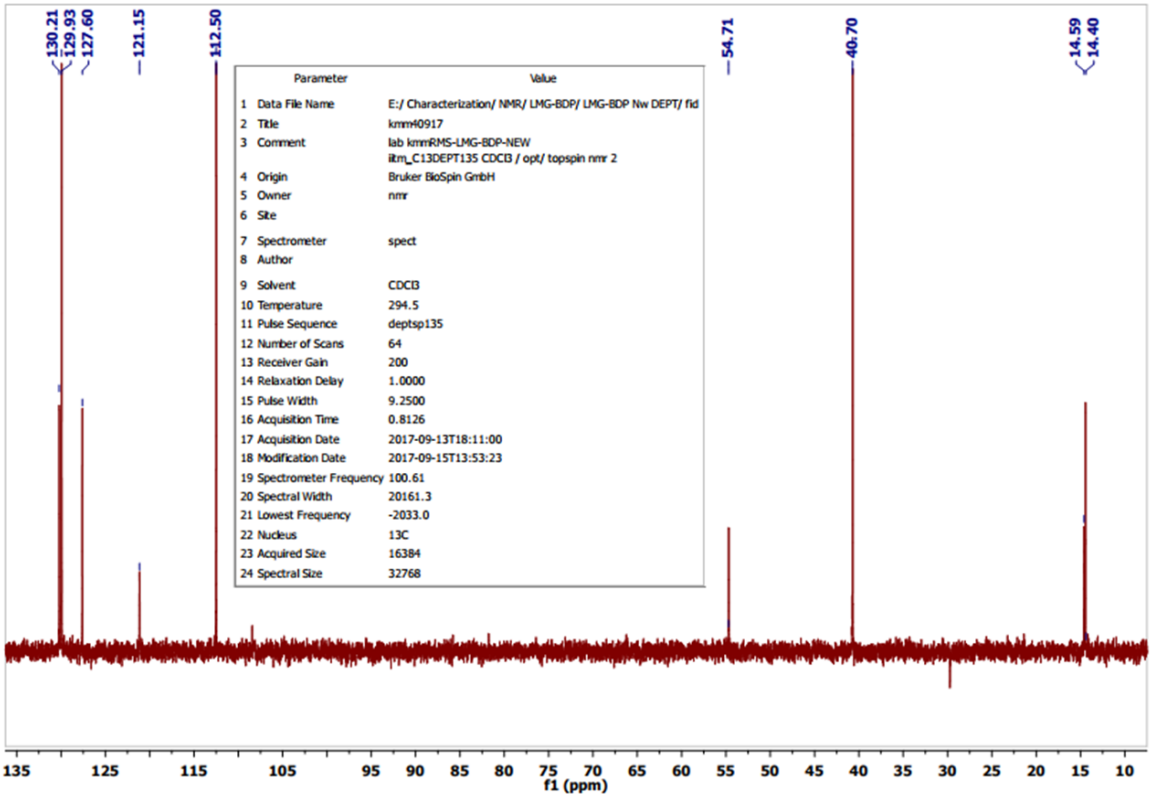

Fig. S38 DEPT-135 of **BDPMBD** (100 MHz, $CDCl_3$).

Data File	LMG.d	**Sample Name**	100119-14-KMM-LMG
Sample Type	Sample	**Position**	P2-B3
Instrument Name	Instrument 1	**User Name**	
Acq Method	Direct Infusion_HPLC.m	**Acquired Time**	10-01-2019 11:03:53 (UTC+05:30)
IRM Calibration Status	Success	**DA Method**	Default.m
Comment			
Sample Group		**Info.**	
Stream Name	LC 1	**Acquisition Time (Local)**	10-01-2019 11:03:53 (UTC+05:30)
Acquisition SW Version	6200 series TOF/6500 series Q-TOF B.08.00 (B8058.0)	**QTOF Driver Version**	8.00.00
QTOF Firmware Version	20.698	**Tune Mass Range Max.**	3200

Compound Table

Compound Label	RT	Mass	Abund	Formula	Tgt Mass	Diff (ppm)	Hits (DB)
Cpd 1: C24 H26 N2 O; 0.573	0.573	358.2064	5176	C24 H26 N2 O	358.2045	5.14	1

Compound Label	m/z	RT	Algorithm	Mass
Cpd 1: C24 H26 N2 O; 0.573	381.1944	0.573	Find By Formula	358.2064

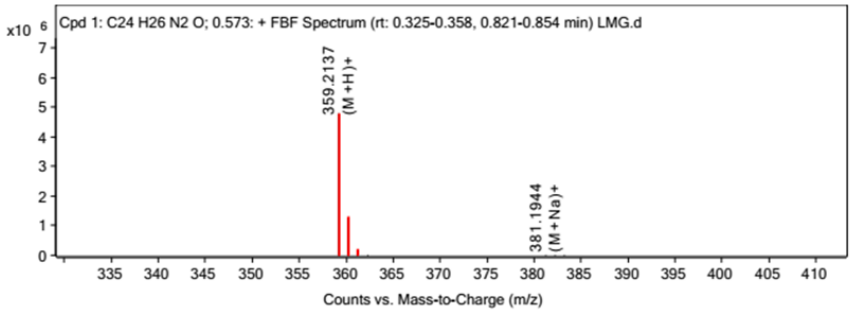

MS Spectrum Peak List

m/z	z	Abund	Ion
359.2137	1	4772866	(M+H)+
360.2165	1	1243241.13	(M+H)+
361.2191	1	145555.81	(M+H)+
362.222	1	11582.34	(M+H)+
381.1944	1	5175.76	(M+Na)+
382.1978	1	1408.94	(M+Na)+
383.2001	1	341.97	(M+Na)+

Fig. S39 Mass spectrum of **LMG-CHO.**

Data File	25IND.d	**Sample Name**	250618-05-KMM-IND
Sample Type	Sample	**Position**	P2-A5
Instrument Name	Instrument 1	**User Name**	
Acq Method	Direct Infusion_HPLC.m	**Acquired Time**	25-06-2018 12:14:06 (UTC+05:30)
IRM Calibration Status	Success	**DA Method**	Default.m
Comment			
Sample Group		**Info.**	
Stream Name	LC 1	**Acquisition Time (Local)**	25-06-2018 12:14:06 (UTC+05:30)
Acquisition SW Version	6200 series TOF/6500 series Q-TOF B.08.00 (B8058.0)	**QTOF Driver Version**	8.00.00
QTOF Firmware Version	20.698	**Tune Mass Range Max.**	3200

Compound Table

Compound Label	RT	Mass	Abund	Formula	Tgt Mass	Diff (ppm)	Hits (DB)
Cpd 1: C35 H37 N3; 0.533	0.533	499.2998	3415605	C35 H37 N3	499.2987	2.04	1

Compound Label	m/z	RT	Algorithm	Mass
Cpd 1: C35 H37 N3; 0.533	500.307	0.533	Find By Formula	499.2998

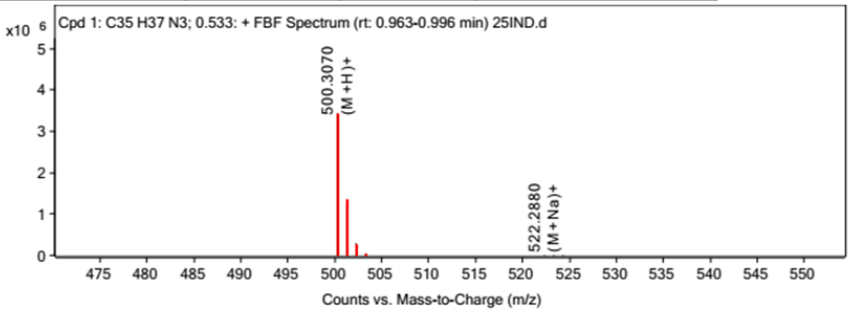

MS Spectrum Peak List

m/z	z	Abund	Ion
500.307	1	3415604.75	(M+H)+
501.3101	1	1239005.38	(M+H)+
502.3146	1	268062.97	(M+H)+
503.3178	1	42443.51	(M+H)+
522.288	1	8049.47	(M+Na)+
523.2904	1	5275.8	(M+Na)+
524.2942	1	4961.48	(M+Na)+

Fig. S40 Mass spectrum of **InMBD.**

Data File	BZI.d	**Sample Name**	030718-3-KMM-BZI
Sample Type	Sample	**Position**	P1-D3
Instrument Name	Instrument 1	**User Name**	
Acq Method	Direct Infusion_HPLC.m	**Acquired Time**	03-07-2018 09:41:33 (UTC+05:30)
IRM Calibration Status	Success	**DA Method**	Default.m
Comment			
Sample Group		**Info.**	
Stream Name	LC 1	**Acquisition Time (Local)**	03-07-2018 09:41:33 (UTC+05:30)
Acquisition SW Version	6200 series TOF/6500 series Q-TOF B.08.00 (B8058.0)	**QTOF Driver Version**	8.00.00
QTOF Firmware Version	20.698	**Tune Mass Range Max.**	3200

Compound Table

Compound Label	RT	Mass	Abund	Formula	Tgt Mass	Diff (ppm)	Hits (DB)
Cpd 1: C39 H39 N3; 0.252	0.252	549.3142	1435818	C39 H39 N3	549.3144	-0.31	1

Compound Label	m/z	RT	Algorithm	Mass
Cpd 1: C39 H39 N3; 0.252	550.3214	0.252	Find By Formula	549.3142

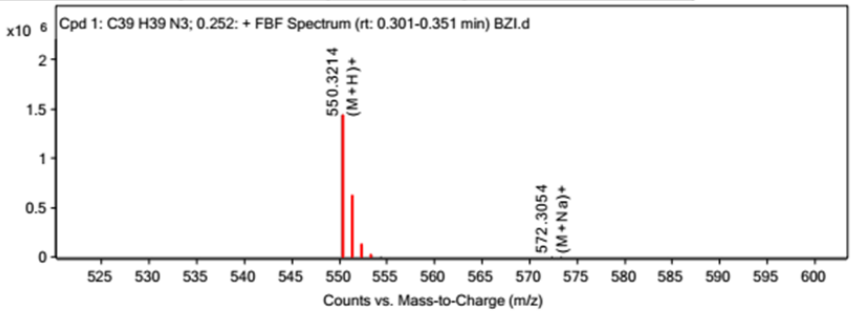

MS Spectrum Peak List

m/z	z	Abund	Ion
550.3214	1	1435817.88	(M+H)+
551.3252	1	557335	(M+H)+
552.3276	1	109794.51	(M+H)+
553.3307	1	15000.29	(M+H)+
554.3329	1	1938.28	(M+H)+
572.3054	1	685.98	(M+Na)+
573.299	1	200.89	(M+Na)+

Fig. S41 Mass spectrum of **BInMBD.**

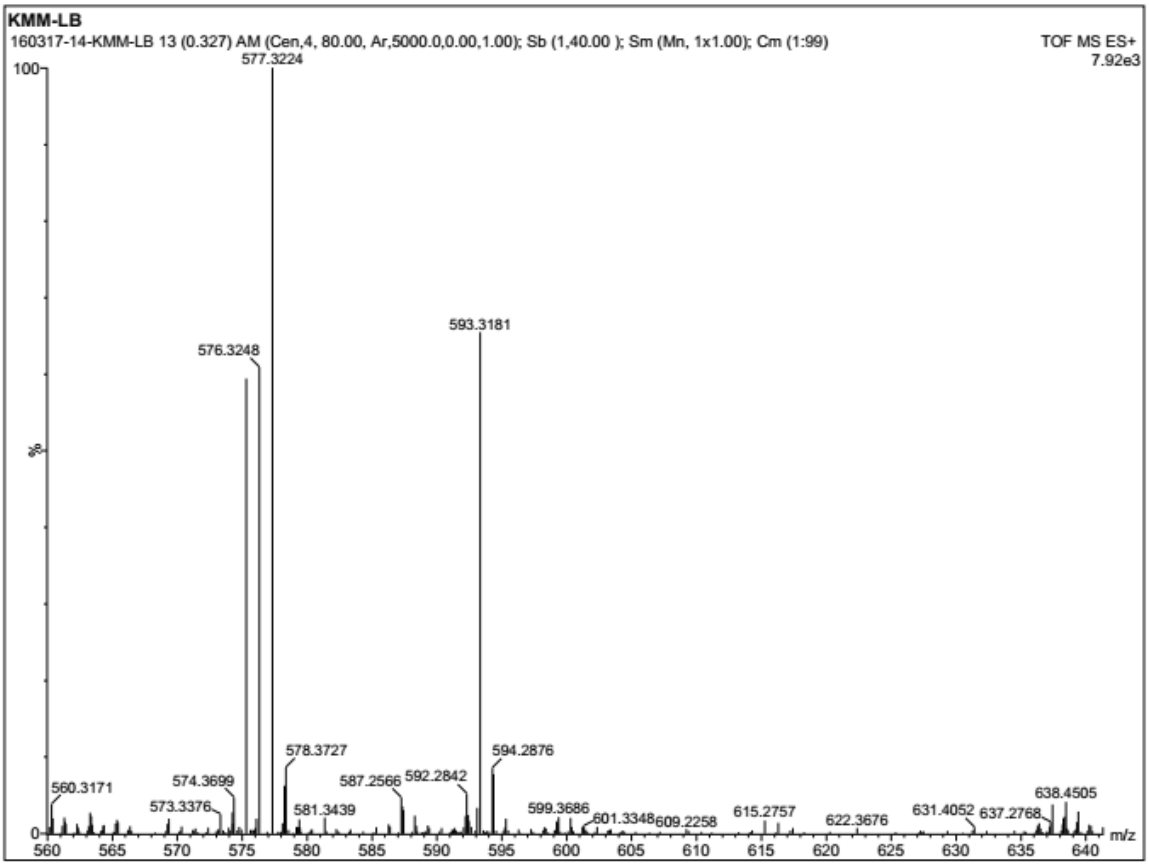

Fig. S42 Mass spectrum of **BDPMBD.**